the shafts and tips of the microelectrodes lie on the same axis, there being no distortion due to gravitational force.

The taper and tip diameter are adjustable by varying such parameters as the heat of the coil, the position of the coil, the distance of the first pull and the magnitude of the second pull. Another advantage is that the machine may be easily constructed in a small workshop from standard parts, steel plate and rod. However it is an advantage to have access to a coil winding machine for the solenoid. Since there is such a small wastage and since both upper and lower tubes are identical, it is possible to pull two useful microelectrodes per minute with this machine.

THE REVIEW OF SCIENTIFIC INSTRUMENTS VOLUME 27, NUMBER 7 JULY, 1956

Cyclotron Instrumentation for Nuclear Spectroscopy at Medium Resolution in Energy*

D. R. Bach, W. J. Childs, R. W. Hockney, P. V. C. Hough, and W. C. Parkinson
Harrison M. Randall Laboratory of Physics, The University of Michigan, Ann Arbor, Michigan
(Received March 29, 1956)

The instrumentation for the magnetic focusing and analysis of the external beam of the Michigan cyclotron is described. It provides to a scattering chamber in an adjacent room a beam of deuterons of a few tenths microampere monoenergetic to within 15 kev at a mean energy of 7.8 Mev. A double-focusing analyzer magnet of mean radius one meter, focuses reaction products of magnetic rigidity less than or equal to that of a 20-Mev proton. At the optimum energy resolution of the system, proton groups from (d,p) reactions differing in Q by about 20 kev can be resolved. Particles can be observed over a continuum of angles from $-7°$ to $+112°$ relative to the incident beam. The determination of reaction energies and the measurement of relative differential cross sections are discussed.

I. INTRODUCTION

In the study of nuclear structure with the aid of nuclear reactions, incident particle energies well above the range of Van de Graaf generators are frequently useful. The use of intermediate energy cyclotrons for such problems has been restricted however by the several-hundred kilovolt spread in energy of a typical cyclotron unresolved external beam.

From the first experiments with the 7.8-Mev external deuteron beam of the rebuilt Michigan cyclotron, the limitations arising from poor resolution in energy were apparent. As an example, the "ground state" proton group from the $P^{31}(d,p)$ reaction studied in this laboratory[1] was resolved by Van Patter *et al.*[2] into two groups differing in Q by 77 kev. It was desirable, therefore, to undertake the magnetic analysis of the external beam and of the reaction products. A first goal of 20-kev resolution at 10 Mev appeared useful and realizable.

With the stripping reactions in mind, provision was made for a continuum of observation angles extending relative to the incident beam from $-7°$ to 112°, the limits in angle being imposed by the size of the scattering room. The system was designed to focus reaction products of magnetic rigidity less than or equal to that of a 20-Mev proton.

A drawing in plan of the cyclotron, its two associated magnets, and the shielding is shown in Fig. 1. The cyclotron room, which also contains the focusing magnet, is shielded from the analyzer room by 30 in. of water. The control room is likewise shielded from the scattering room by 30 in. of water.

II. BEAM PREPARATION

Characteristics of the External Beam

In stable operation the cyclotron yields between 50 and 150 μa of 7.8-Mev deuterons outside the dees. The cross section of the beam at the exit window extends about 3 cm radially and less than 2 cm vertically. Sometimes two peaks appear in the vertical intensity distribution, perhaps owing to a slight central obstruction at the cutting edge. The variations observed are probably due to changes in the phase of the vertical and radial oscillations of the ions at extraction.[3,4]

Of the total current available outside the dees only 5 to 15 μa can be induced to enter the vacuum duct leading to the focusing magnet, owing to the now-obsolete design of the main vacuum chamber which was constructed in 1939. In compensation for this disadvantage some energy resolution is effected in the cyclotron fringing field. The energy spread in the duct beam is about 100 kev, as measured by the lateral dispersal of the beam by the focusing magnet.

The vertical motion of the external beam is controlled by an electrostatic field between plates approximately 5 cm apart and 1 m long in the duct. A maximum

* This work was supported in part by the U. S. Atomic Energy Commission and by the Michigan Memorial-Phoenix project.
[1] Parkinson, Beach, and King, Phys. Rev. 87, 387(L) (1952).
[2] Van Patter, Endt, Sperduto, and Buechner, Phys. Rev. 86, 502 (1952).
[3] Beach, Childs, Hough, King, and Parkinson, Phys. Rev. 86, 582(A) (1952).
[4] P. V. C. Hough, Rev. Sci. Instr. 24, 42 (1953).

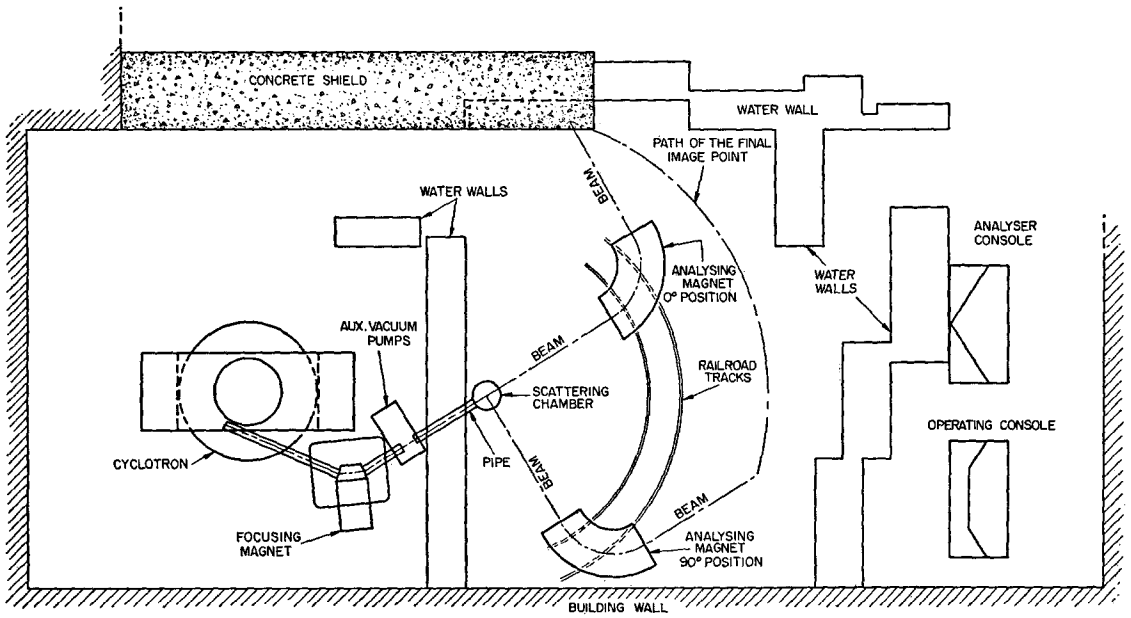

FIG. 1. Plan sketch of the cyclotron and its associated instrumentation.

potential difference of 10 kev between the plates provides sufficient deflection. The plates can also be pulsed to allow one bunch of ions, of time duration less than 5 mμsec to pass through the focusing magnet.[5]

In the design of the focusing magnet it was considered important not to assume that the beam issues from the cyclotron as from a point source. Therefore a radial slit was installed at the exit window. The machine "illuminates" the slit, and the focusing magnet images the slit at the center of the scattering chamber. The beam resolution is thus calculable and depends only on the quality of the focusing magnet. For intensity reasons the slit was placed as close to the exit of the deflector channel as possible.

The Focusing Magnet

The magnet for focusing and analyzing the beam is a 50° wedge with $n \equiv (r/H)(dH/dr) = 0.2$. It is constructed in the form of a "C" with the current coils above and below the gap. The coils are rectangular pancakes wound with $\frac{1}{16} \times 1$-in. copper strap. Water cooling is accomplished by inserting between each pair of coils a $\frac{3}{8}$-in. thick copper plate having $\frac{1}{4}$-in. copper tubing soft-soldered into grooves milled in S curves in the surface. The coils are insulated between turns with paper tape, and from the cooling plates by $\frac{1}{16}$-in. Consoweld MP-16 plastic sheets.[6]

Power to the magnet is supplied at 50 volts and 120 amperes by a dc generator. The magnet current is regulated at present with a circuit of the Lawson design.[7] With this arrangement the average beam energy on the target is held constant to within about 5 kev over several hours.

The performance of the focusing magnet showed little correspondence with the theory,[8,9] probably because the ion path length in the fringing field is an appreciable fraction of the path length in the magnet proper. The magnet was originally constructed with $n = 0.5$, but to achieve an image position required by the room geometry, it was necessary to reduce n to 0.2. The vertical focusing has not been investigated experimentally, but for this value of n, the theory predicts that the deuterons emerge from the field with zero vertical component of velocity.

The general characteristics of the magnet are listed in Table I.

The Stretched-Wire Technique for Establishing a Radial Focus

The duplication of particle trajectories by a stretched current-carrying wire has often been used in correcting

TABLE I. Focusing magnet characteristics.

Radius of curvature	45 cm
Wedge angle	50°
Beam deflection angle	55°
Magnetic field fall-off parameter, n	0.2
Object distance	171 cm
Image distance	228 cm
Dispersion	6.5 kev/mm at 8 Mev
Width of the image of a monoenergetic line source	2–3 mm
Magnet gap (average)	5.7 cm
Corrected field horizontal aperature	14 cm
Average gap field	9000 gauss

[5] R. Grismore and W. C. Parkinson (to be published).
[6] Obtained from Consolidated Water Power and Paper Company, Wisconsin Rapids, Wisconsin.
[7] J. L. Lawson and A. W. Tyler, Rev. Sci. Instr. 10, 304 (1939).
[8] D. Judd, Rev. Sci. Instr. 21, 213 (1950).
[9] E. S. Rosenblum, Rev. Sci. Instr. 21, 586 (1950).

magnetic lenses. The tension in the wire is ordinarily established by passing the wire over a wheel to a weight pan. Often an important limitation in the precision of the measurement arises from the unknown and variable tension introduced by frictional torque at the wheel bearings. In correcting the field of the focusing magnet it was found that frictional effects could be effectively eliminated by substituting for conventional bearings tungsten needle points resting on gently curved glass supports, and in addition vibrating the wire gently by passing it through a small auxiliary 60-cps magnetic field. Under these conditions, and with the currents for both the magnet and the wire regulated, the direction of the wire as it left the field of the focusing magnet could be determined to within about 2′ of arc. This angular uncertainty corresponds to a 1-mm uncertainty in lateral position of an ion at the image position approximately 2 m beyond the exit face of the magnet.

The source point of the stretched wire was established at the exit slit of the cyclotron. The cyclotron magnetic field was maintained at the deuteron resonance value and all magnetic shielding later to be used for the beam was installed. In this way the stretched-wire measurement took account of all accidental lenses in the beam path.

The angle of the wire after leaving the focusing magnet was measured by passing it over two points rigidly connected to the graduated rotating table of an optical spectrometer. For perfect focus, this angle should vary linearly with the lateral displacement of the wire across the exit aperture of the magnet in the approximation, valid for this case, of small angular aperture. The slope of the graph of wire angle *vs* lateral displacement is the reciprocal of the distance to the image.

For rough correction of the magnetic field, banks of $\frac{1}{2}\times 2\times\frac{1}{4}$-in. iron shims were clamped against the sides of the pole tips at the entrance aperture and also at the exit. By tapping groups of these shims closer to or farther from the gap, the total deflection of an ion passing under the shims could be adjusted. When the field was roughly corrected the banks were replaced with a single $\frac{1}{2}$-in. iron plate cut to the indicated contour. The final correction of the field was made using a row of horizontal iron screws at the exit face of the magnet. To increase the field at a given point across the aperture, the appropriate screws were brought closer to the pole piece.

Using this technique the field was corrected until an energy spread of 20 to 30 kev at one point in the image plane was indicated by the stretched wire. Since at this time little confidence was placed in the accuracy of the method, further correction was planned using the deuteron beam itself. Actually, as described below, the combined spread in energies due to ion optical imperfections in both the focusing magnet and reaction products analyzer magnet was found to be only 20 kev. The combination of the stretched-wire measurements with these results imply that less than the full aperture of the focusing magnet is used and that the beam, over an area 1 mm wide by 1 cm high at the image plane is monoenergetic to within about 15 kev.

The dispersion of the magnet is easily determined by altering the current in the stretched wire, with the result shown in Table I. The width of the image of a monoenergetic line source quoted in Table I is obtained by combining the dispersion measurement with the observed 15 kev energy spread in the deuteron beam at one point in the image plane.

The total deuteron beam delivered to the scattering chamber by the focusing magnet is 2 to 6 μa while that within a 15 kev range of energy is approximately 0.3 μa.

Limitations of the Present Arrangement

While the energy of the resolved incident beam, measured as described in Sec. VI, remains constant to within about 5 kev during any one run it has been found to vary as much as 140 kev between runs. To remove this variation, presumably due to hysteresis in the iron, the magnetic field of the focusing magnet is to be regulated rather than the current in the magnet coils. A fine control on the cyclotron oscillator frequency has been installed and is used to maximize the beam intensity at the energy determined by the focusing magnet. With the magnetic field stabilized to a prescribed value the resolved beam energy will be accurately reproducable.

The mean angle of incidence of the beam has been found to vary by as much as 1°. Convenient procedures for monitoring the angle have not yet been worked out.

A significant increase in the total as well as resolved beam intensity at the scattering chamber is expected on installation of a new tank.

III. THE SCATTERING CHAMBER AND GENERAL VACUUM TECHNIQUE

The Scattering Chamber

A scattering chamber should permit a continuous variation of the angle of observation under vacuum without the interposition of windows. The solution adopted is shown in the line drawing of Fig. 2. The incident beam enters through the port on the lower corner of the tipped cylindrical box. The exit port is rigidly attached at the corner of the rotating lid, so that at the 0° position of the lid the beam passes along a diagonal of the box and directly through the port. A ball bearing race between the lid and box supports the vacuum load on the rotating lid and a large O-ring provides the vacuum seal.

Without further mechanism the exit port would rise above the horizontal plane at angles other than 0°.

To prevent this the entire chamber is mounted on bearings so that it may rotate around the axis of the beam, and a track is used to constrain the exit port to the horizontal plane. To prevent the beam-axis bearing from interfering with the motion of the port the front bearing circle is made large in diameter with a U-shaped slot cut into both fixed and moving members of the bearing.

The target assembly and beam monitor counters are supported and held fixed in space by a pipe which enters the chamber from the rear along the beam line. Provision is made for rotating several targets into the path of the beam, and for substituting at the target position a thin polonium source, in each case without breaking the vacuum. Figure 3 is a photograph of the interior of the chamber, showing a target in place, and the double proportional counter used for a beam monitor.

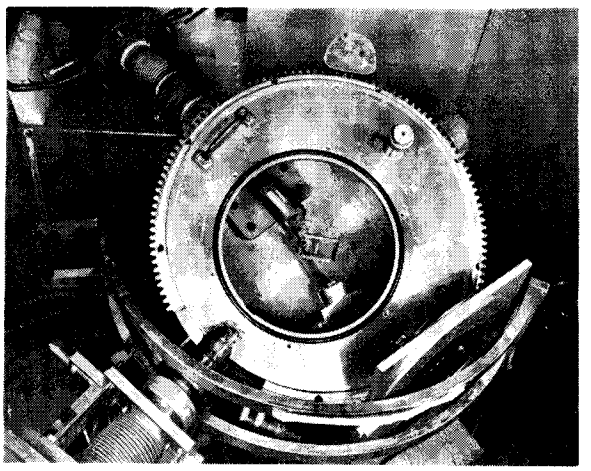

FIG. 3. Top view of the scattering chamber showing the monitor counter and a target in place.

Vacuum Technique

The evacuated space of the over-all system may be separated by large clapper valves into three regions, each with its own diffusion and mechanical pumps. The first region comprises the cyclotron tank and the ductwork through the focusing magnet. Whenever the deuteron beam is not being used in the scattering chamber, region I is isolated as a precaution against vacuum accidents. Region II consists of the scattering chamber and portions of the ductwork from the focusing magnet to the analyzer magnet and region III the analyzer vacuum chamber and ductwork to the image plane of the reaction products. Ordinarily, regions I and III are maintained at high vacuum, and the transitions to atmospheric pressure required for target changes are confined to region II. For exposure of nuclear emulsions inside the vacuum at the final image plane and for coupling on thin window counters, region III alone is let down, so that a fragile target in region II need not be disturbed.

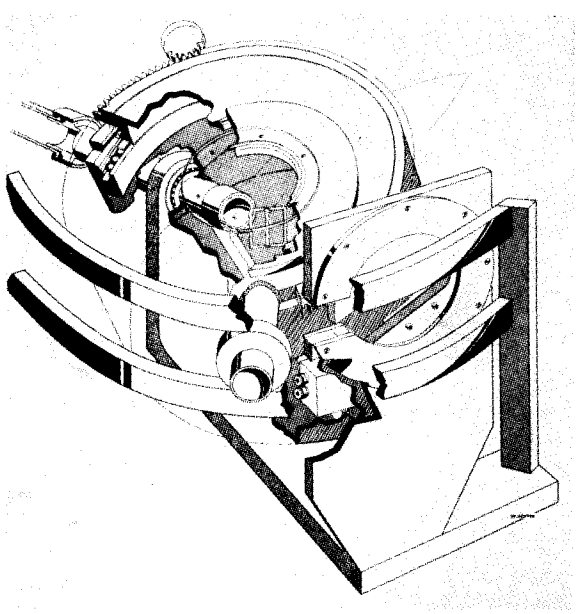

FIG. 2. Cutaway drawing of the scattering chamber.

The pressure in region I is maintained at $1\text{–}3\times10^{-6}$ mm Hg. In regions II and III the pressure is ordinarily less than 1×10^{-5} mm Hg, so loss of resolution from gas scattering[10] is negligible. The pumps for each of the three regions are individually protected against vacuum failure by d'Arsonval movement relays used with standard thermocouple gauges.

IV. REACTION PRODUCTS ANALYSIS

The Analyzer Magnet

The reaction products analyzer magnet, shown in Fig. 4, was assembled from a quarter circle of spare H sections from the Michigan synchrotron. The original pole-face contour, designed to increase the region over which n is constant, and thus increase the useful radial aperature[11,12] was milled off and new plane steel pole tips fastened to each section. The pole tips were extended in azimuth to reduce to zero the space between the H sections at the gap, and to reduce the mean gap height from $3\frac{1}{2}$ in. to 6 cm. The useful region of the field was then extended radially by sliding annular iron shims into pockets prepared in the top and bottom of the magnet vacuum box. Using the stretched-wire technique, trial-and-error adjustment of the annular shims yielded an aperture of 4 in. for which the image of a monoenergetic point source was diffused laterally by less than 1 mm.

The mean radius of curvature of 1 m allows 20-Mev

[10] For reaction protons of energy greater than 1 Mev, single scattering is most important. See E. Segrè, *Experimental Nuclear Physics* (John Wiley and Sons, Inc., New York, 1953), p. 249 ff.

[11] Parkinson, Grover, and Crane, Rev. Sci. Instr. **18**, 734 (1947).

[12] K. Siegbahn and Svartholm, Arkiv. Mat. Astron. Fysik **33A**, No. 21 (1946).

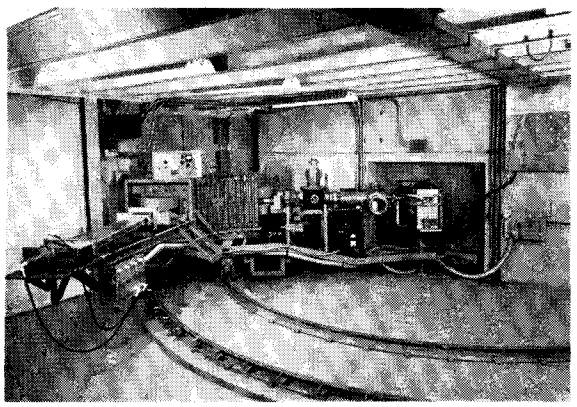

FIG. 4. General view of the scattering room showing the scattering chamber (right corner) and the analyzer magnet.

protons to be focused with a gap field of only 6500 gauss, so that the iron is always well below saturation. A fall-off parameter of $n=0.45$ was chosen to provide as much vertical focusing as was consistent with keeping the radial image position within the room.

Because of the low flux density and the relative unimportance of the fringing field, the analyzer magnet performance agreed closely with the first-order theory.[8,9]

The magnet coils and cooling plates are similar in construction to those of the focusing magnet. The analyzer field is regulated by a commercial proton moment field control[13] which is connected through a dc amplifier to power tubes in series with the field of the magnet generator. With this arrangement the mean energy of particles entering a detector fixed at the image plane is stable to within about 5 kev for many hours, and over a wide range of incident particle energies. The proton resonant frequency is read very conveniently with a Hewlett-Packard frequency meter.[14]

The characteristics of the analyzer magnet are listed in Table II.

Magnet Motion

The analyzer magnet is mounted on a steel box-frame carriage which rolls on carefully leveled rails laid in circular arcs. Integral members of the box frame run to a 3-in. barrel bearing mounted on a vertical shaft sunk in concrete directly under and centered on the scattering chamber. In this way the distance of the magnet from the axis of rotation is held fixed to within a millimeter and in particular is independent of the shape of the rails. To avoid systematic errors the axis of rotation and the target center are carefully aligned. The axis was determined by extending an arm, rigidly attached to the magnet, through the target area and locating the point of minimum motion as the analyzer magnet was rotated.

A displacement of the target from the axis of rotation introduces systematic deviations in the solid angle subtended by the analyzer, in the scattering angle, and in the energy of a particle group brought to a focus at a fixed line in the image plane. Only the last effect is important. If the target is off-axis by a distance ϵ at an angle ϕ relative to the incident beam direction, and θ is the angle of observation, the change in mean energy of particles entering a detector fixed at the image plane is $\Delta E=d\cdot\epsilon\cdot\sin(\theta-\varphi)$, where d is the change in energy per mm displacement in the image plane for the energy in question. For a particle energy of 8 Mev, $d\simeq 4$ kev/mm, so that energy shifts of ± 4 kev are produced by an error $\epsilon\sim 1$ mm.

Zero angle for the system was determined by slitting the analyzer aperture nearly to zero and adjusting the magnet position until the incident beam passed through. The very high intensities encountered at the final image plane were conveniently measured by running the beam into an aluminum plate which was shielded by lead except for a narrow vertical strip at the center. Counters, nearby, detected the radiation from the aluminum.

The final image circle has a radius of 172 in. The analyzer carriage, driven at one of its wheels, operates the scattering chamber motor through a master-slave microswitch arrangement located at the flexible vacuum coupling between the two systems. Projections adjacent to the outer rail activate microswitches attached to the carriage which stop the magnet automatically at 5° intervals. The angular coordinate system is internally consistent to within 0.1°, but as mentioned above the incident beam direction can change by as much as 1°. A remote-control and indicator system allows the magnet to be moved with the beam on.

Ion Optics

The combined focusing and analyzer magnet system was tested by studying the "line" of deuterons elastically scattered at 10° from a gold leaf strip 2 mm wide, placed at the image plane of the focusing magnet. With both magnetic fields held fixed a 2-mm slit was driven laterally across the analyzer image plane in front of two proportional counters in coincidence.

TABLE II. Analyzer magnet characteristics.

Radius of curvature	100 cm
Deflection angle	90°
Fall-off parameter, n	0.45
Object distance	208 cm
Predicted image distance	202 cm
Measured image distance	208±5 cm
Central dispersion	4 kev/mm at 8 Mev
Width of an image of a point monoenergetic source	1 mm
Average magnetic gap	6 cm
Geometrical horizontal aperture	17 cm
Corrected field horizontal aperature	10 cm
Maximum gap field	6500 gauss
Solid angle	6×10^{-4} sterad

[13] Model V-4400, Varian Associates, Palo Alto, California.
[14] Model 524A, Hewlett-Packard, Palo Alto, California.

At this point it should be noted that the focusing and analyzer magnets bend the paths of the particles in the same sense, and since the analyzer image is inverted radially, the dispersions of the two systems subtract. With perfect ion optics, the spread in deuteron energy across the gold strip would be 12 kev. The dispersion of the analyzer at the given deuteron energy is 4 kev/mm. Therefore instead of a radially inverted 2-mm-wide image of the gold strip at the final image plane, a 1-mm-wide image, without radial inversion, is expected. [For (d,p) reactions of moderately positive Q the dispersions nearly cancel, and quite wide targets can be used.]

In the test of the two magnets using the deuteron beam, therefore, the spread of the final image is due almost entirely to ion-optical imperfections. The line shapes obtained for elastically scattered deuterons with analyzer radial apertures of 4 in. and 7 in. are shown in Fig. 5. The low-energy tail apparent with the 7-in. aperture implies that the field has been overcorrected at the edges of the gap.

The analyzer image distance was located by measuring the line shape for a sequence of distances of the slit from the magnet face. The vertical focusing of the analyzer has not been investigated in detail. It is known that the vertical size of the image of a point scatterer is appreciably less than 1 cm.

For a given setting of the analyzer magnet field, a 15% range of reaction product energies is dispersed over a lateral distance of 30 cm at the image plane. Of

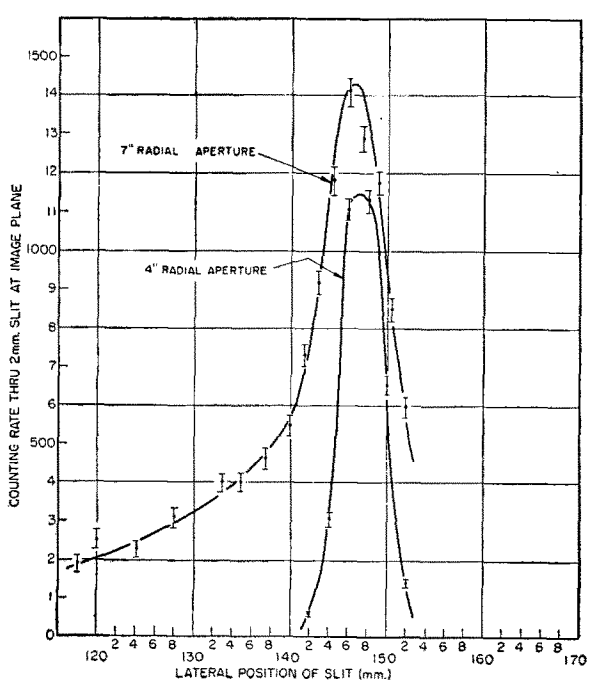

FIG. 5. Line shapes obtained for elastically scattered deuterons with analyzer radial apertures of 4 in. and 7 in. The low-energy tail apparent for the 7-in. aperture implies that the analyzer field has been overcorrected at the edges of the gap.

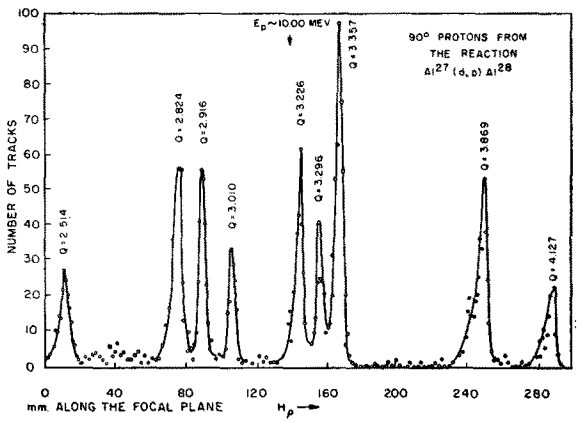

FIG. 6. Proton spectrum obtained in the $Al^{27}(d,p)Al^{28}$ reaction.

primary interest in the measurement of energies is the quantity $\rho(x)$, the ratio of the momentum of a particle focused at a position x in the image plane, to the momentum focused at a standard position, say the midline. The quantity $\rho(x)$ has been determined experimentally by recording on photographic plates placed at the image plane a portion of the proton spectrum from the reaction $Al^{27}(d,p)Al^{28}$.[15] A typical record is shown in Fig. 6; its use in the determination of ρ is discussed in Sec. VI. It is found that ρ is distinctly nonlinear in x, owing to second-order corrections[16] to the path of an ion which travels far from the central ray. Such ions are principal contributors to a group focused at the edge of the useful region of the image plane. While it would be useful to calculate the necessary second-order corrections, they depend in an essential way on the curvature in the plot of the magnetic field intensity *vs* positions across the magnet aperture, and this has not been measured.

In order to make best use of the corrected field region in the analyzer a stop of 4-in. radial aperture was installed at the mean azimuthal angle of the magnet. Even then the quality of focus deteriorates significantly in going from the midpoint to the edge of the image plane. In Fig. 6, the half-width of a central porton group is 20 kev at 10.1 Mev, and while the half-width of the far right-hand group is 22 kev at 11.0 Mev, the quality of focus, as evidenced by the low-energy tail, has deteriorated. At the far left, the single peak arises from a doublet separated in energy by 26 kev. The doublet would just be resolved at the center of the image plane if the groups were of nearly equal intensity.

The quality of focus lost at the edge of the image plane may be recovered in part by proper orientation of the plane of the detectors. Thus far detectors have been arrayed in a plane perpendicular to the central ray. The first-order theory predicts an image plane

[15] P. M. Endt and J. C. Kluyver, Revs. Modern Phys. **26**, 95 (1954), and references therein.

[16] F. B. Shull and D. M. Dennison, Phys. Rev. **71**, 681 (1947), and **72**, 256 (1947).

oriented at ~60° to the perpendicular, with low-energy particles focused closer to the magnet. Because of the importance of second-order corrections the plane of best focus is to be located experimentally.

V. DETECTORS

The two types of particle detectors which have proved to be the most satisfactory for use at the analyzer image plane are the double proportional counter telescope and the nuclear emulsion.

For rapid surveys and for measurements on relatively strong groups the counter telescope is particularly useful. With the analyzer exit window closed and the cyclotron in operation the background coincidence rate is 1 count per hour or less. Equipped with a 1.7-mg/cm^2 Mylar window, such a counter will detect reliably protons of energy greater than 1 Mev. A double counter of stopping power less than 100 μg/cm^2 has been constructed for particles of shorter range.

A high flux of deterons occurring at the same momentum as a weak proton group is readily eliminated by absorbing foils. In the converse situation, the deuterons are distinguished without ambiguity by their pulse height, which is four times that of the protons. In general, the pulse height in a proportional counter due to a particle of mass M, charge Z and momentum p is approximately proportional[17] to Z^2M^2/p^2. Since the magnet at a given field fixes Z/p the pulse heights are proportional to the square of the mass of the particle and are independent of the charge. Occasionally it is desirable to measure simultaneously a spectrum of (say) deuterons and protons. It is convenient then to record the pulses of one of the pair of counters with a multichannel analyzer which is gated by the other; the proton and deuteron counts then appear in widely separated channels.

The photographic plate is particularly useful for measurements on weak groups and for covering a larger range in momenta. A 1×12-in. plate at the image plane will register at one time reaction products over a fractional momentum range of 0.075. At maximum resolution one plate is equivalent to about 100 counter pairs. The disadvantage of the relatively long plate scanning time is frequently more than compensated for by the reduction in cyclotron running time.

Scintillation counter crystals cannot easily be made thin enough to get coincidence detection, and even NaI(Tl) discriminates less effectively than do proportional counters against the background arising from the large flux of neutrons from the cyclotron.

VI. ENERGY MEASUREMENTS

The Analyzer Magnet Fluxmeter and its Calibration

In order to determine the absolute kinetic energies of the incident deuterons and the reaction products it is necessary that an absolute energy scale be established for the reaction products analyzer magnet. The incident beam energy is then readily determined by measuring the kinetic energy of deuterons elastically scattered from a known target nuclide, preferably one of high mass. The first requirement in establishing the energy scale is a fluxmeter whose indication is uniquely related to the momentum of particles focused at the midline of the image plane. This has been met by installing a nuclear moment fluxmeter directly in the magnet gap. The magnetic field across the fluxmeter sample was made uniform by locating the sample at the point of maximum field near the inner edge of the radial aperture and by constricting slightly the gap on either side of the sample. Measurements indicate a reproducibility in the measurement of particle momenta of better than 0.03%.

An absolute energy calibration will be made using the alpha particles from polonium 210.[18] The linearity of the effective $H\rho$ *versus* fluxmeter reading of the analyzer magnet will be tested by the energy-angle relationship in the elastic scattering of deuterons from light nuclei.

As an alternative to the use of Po alpha particles, the energy calibration may be made in terms of a well-established Q of a (d,p) reaction. The method is as follows.[19] For certain light target nuclei, the Q of the (d,p) reaction insures that at some angle of observation the proton momentum is equal to the momentum of the deuteron elastically scattered by the same nuclide. Evidently the equal-momentum angle depends on the beam energy, and therefore can be used to measure it, for if at this angle the beam energy were to increase by 2%, the scattered deuteron momentum would increase by 1%, while the proton momentum would increase by about ½%. Therefore it would be necessary to observe at a larger angle to re-establish the condition of equal momenta. In practice, the momenta need be only approximately equal, provided both the protons and deuterons are brought to a focus on a single photoplate and provided the dispersion of the magnet is moderately well known. A formula is given below for the calculation of the deuteron energy E_1, in terms of the angle of observation, the separation of proton and deuteron groups on the photoplate, and the Q of the reaction.

For a target nucleus of mass number A, the minimum absolute error in the beam energy determination is approximately $(A+2)/(A-2)$ times the absolute error in the Q. Reactions which have suitable and well-known Q's are: $Li^6(d,p)Li_0^7$, $B^{10}(d,p)B_1^{11}$, and $C^{13}(d,p)C_0^{14}$, where the subscripts indicate that the reaction proceeds to the ground or first excited state.

[17] M. S. Livingston and H. A. Bethe, Revs. Modern Phys. **9**, 245 (1937).

[18] G. H. Briggs, Revs. Modern Phys. **26**, 1 (1954).

[19] The method was proposed by Bach and Hockney, and has been demonstrated experimentally by Bach.

Expression of an Unknown Q in Terms of a Comparison Q^* and Directly Measured Quantities

The most valuable nuclear energy measurements are certainly those related directly to an easily reproducible standard energy such as that of a polonium alpha particle. However, it is often convenient to refer an unknown Q to the Q^* of a comparison group of particles of approximately the same momentum. The comparison is frequently insensitive to uncertainties in the incident beam energy and angle, and in advance of our complete knowledge and control of these quantities for the external cyclotron beam, we have relied extensively on such measurements.

The linear separation of unknown and known particle groups at the analyzer image plane yields a measurement of the ratio r of the relativistic momenta of the two groups. Using the notation of Brown *et al.*[20] (hereafter referred to as B), and denoting quantities relating to the comparison reaction with *, the relationship may be written as $P_2=rP_2^*$. If in Eq. (A11″) of B, P_2 is eliminated in favor of P_2^*, Q may be expressed in terms of Q^*, E_1 and θ^*, by the use of Eq. (A12) of B. The known and unknown reaction angles are not quite equal, because particles arriving at different positions in the image plane take different paths through the magnet. The relation may be expressed as

$$\theta=\theta^*-(r-1)\beta,$$

in which $\beta=0.23\pm0.05$ radian is a dimensionless parameter determined by tracing alpha particles through the magnet and has the significance of change in reaction angle per unit fractional change in momentum, for fixed analyzer magnetic field.

The result of these considerations is the following formula for Q in terms of the comparison Q^*, the measured momentum ratio r, the incident beam energy E_1 at the midplane of the target foil, the comparison reaction angle θ^*, and certain mass ratios.

$$Q=r^2qQ^*+(R+\Theta)E_1+T, \tag{1}$$

$$R=\frac{M_3-M_1}{M_3}(\lambda r^2-1), \tag{1a}$$

$$\Theta=2m\cos\theta^* r\left[(\nu r-1)-(r-1)\beta\tan\theta^*\right]\left[\left(\frac{M_3^*\cdot Q^*}{M_3\cdot E_1}+\frac{M_3^*-M_1}{M_3}+(m\cos\theta^*)^2\right)^{\frac{1}{2}}+m\cos\theta^*\right],$$

$$r=\frac{P_2}{P_2^*},\quad \nu=\frac{M_2^*}{M_2}\cdot\frac{M_3+M_2}{M_3^*+M_2^*},\quad m^2=\frac{M_1M_2^*}{M_3(M_2^*+M_3^*)},$$

$$\lambda=\frac{M_3^*-M_1}{M_3-M_1}\cdot\nu,\quad q=\frac{M_3^*}{M_3}\cdot\nu. \tag{1b}$$

As discussed in B each mass is a "relativistic effective mass," i.e., a nuclear rest mass increased by *half* the kinetic energy expressed in mass units. With this understanding, (1) is correct relativistically. The term T is a correction for target thickness, and may be written

$$T=\left(\epsilon_2-r^2\cdot\frac{M_2^*}{M_2}\cdot\epsilon_2^*\right)\times\left[1+\frac{M_2}{M_3}\left(1-\left(\frac{M_1E_1}{M_2E_2}\right)^{\frac{1}{2}}\cos\theta^*\right)\right], \tag{1c}$$

where ϵ_2 is the energy loss for the unknown group, ϵ_2^* for the comparison group, in half the target thickness as measured along a line in the direction θ^*.

Equation (1) has been checked by extensive comparison with Q values calculated in the usual more direct but more laborious way. Moreover it reduces to a formula given by Peterson, Fowler, and Lauritsen[21] in the special case considered by them.

The notation of (1) is intended to show the terms through which uncertainties in the input data (Q^*, r, θ^*, and E_1) are propagated most sensitively. Thus an uncertainty in r ordinarily introduces the largest error in Q through the term R. (Precise error formulas are easily derived from (1) but have not been found more convenient than carrying an original uncertainty through the calculation.)

For the design of comparison experiments, it may be useful to list some qualitative conclusions which follow from the analysis of Eq. (1).

1. *Effect of an Error in Q^**

If the unknown and comparison groups are both protons or both deuterons, the absolute error in Q is about equal to the absolute error in Q^*. If an unknown deuteron group is compared to a known proton group, the error in Q is about half the error in Q^*. For unknown protons and known deuterons, the error in Q is about twice the error in Q^*.

2. *Effect of an Error in E_1*

If deuterons are compared with deuterons, or protons with protons, the error in Q is slightly less than $(R+\Theta)$ times the error in E_1, and ordinarily negligible. If an unknown deuteron group is compared with a known proton group, about half the uncertainty in E_1 appears in Q, and in the converse situation the whole uncertainty.

3. *Effect of an Error in θ^**

The error in Q introduced by an uncertainty in the reaction angle is a rapidly decreasing function of the masses of the target nuclei, and in addition for $r=1$

[20] Brown, Snyder, Fowler, and Lauritsen, Phys. Rev. 82, 159 (1951), Appendices A, B, and C.

[21] Peterson, Fowler, and Lauritsen, Phys. Rev. 96, 1250 (1954), the un-numbered formula, p. 1257.

contains the factor $(M_2^*/M_2)-(M_3^*/M_3)$. Thus, for reduction of a dominant error due to an uncertainty in θ^* the comparison and unknown target nuclei masses should be chosen in the ratio of the masses of the light particles from the reactions.

4. Effect of an Error in r

An error in r may arise as a result of either imperfect knowledge of the dispersion of the magnet, or through errors in the measurement of peak separations. For the analysis of the errors (only) a constant magnet dispersion k may be assumed, defined by

$$\frac{\delta P}{P}=k\cdot\delta x. \tag{2}$$

Here P is the momentum of a particle focused at the lateral position x in the image plane. Measurements yield the value $k=2.71\times10^{-4}$ mm^{-1} at the image plane midline, but numbers 10% larger and smaller at the high- and low-energy limits, respectively. It follows from (2) in lowest order that

$$\frac{P-P^*}{P^*}=r-1=k(x-x^*).$$

Hence the error in r may be written

$$\delta r=\delta k(x-x^*)+k\delta(x-x^*).$$

At present an uncertainty δk exists which is $\sim10^{-2}k$. If $\xi=\delta(x-x^*)$ represents the uncertainty in the measurement of the unknown and comparison peak positions,

$$\delta r=(2.7\times10^{-4})\left(\frac{x-x^*}{100}+\xi\right), \tag{3}$$

where $x-x^*$ and ξ are expressed in mm. Typically $\xi=1$–2 mm, and $x-x^*$ may be any part of the 300 mm available at the image plane.

The error in Q corresponding to an error δr is $(\partial Q/\partial r)\cdot\delta r$. Although accurate values of $(\partial Q/\partial r)$ may be obtained easily from (1), it is useful to note that in the infinite target mass approximation $(\partial Q/\partial r)=2E_2$. Then a nearly optimum comparison for which $\delta r=5\times10^{-4}$ yields $\Delta Q=10^{-3}E_2$; i.e., with the present resolution, the minimum error in Q, in kilovolts, is roughly equal to the reaction product energy in Mev. Evidently it is preferably to work with negative Q reactions (e.g., the d,d' reactions) when a given state can be reached in several ways, provided the error due to r is dominant.

Throughout, the absolute rather than relative errors in Q have been emphasized because frequently the energy of excitation of a state is the quantity of interest and this energy follows from Q differences.

Determination of the Image Plane Dispersion Function $\rho(x)$

The function $\rho(x)$ has been defined in Sec. IV as the ratio of the relativistic momentum of a particle focused at the lateral position x in the image plane to that of a particle focused at the image plane midline. Once ρ is determined, the momentum P_2 of an unknown group of particles focused at x may be found from the known momentum P_2^* of a comparison group focused at x^* by the relation

$$(P_2/P_2^*)=\rho(x)/\rho(x^*).$$

This ratio is the quantity r of Eq. (1).

In Fig. 6 the Q's of the reaction groups have been labeled (from right to left) C, D, $E_{1,3,2}F_{2,3,1}G_{1,2}$ by Enge, Buechner, and Sperduto,[22] and have been measured by them to an accuracy of 4 to 6 kev. (In our spectrum, the groups $G_{1,2}$ are unresolved.) If any one of the groups is called j, any other i, and $r_{ji}\equiv P_{2j}/P_{2i}\equiv\rho(x_j)/\rho(x_1)$, Eq. (A12) of B, for $\theta=90°$ yields

$$r_{ji}^2-1=\frac{Q_j-Q_i}{(M_3-M_1/M_3)\cdot E_1+Q_i}. \tag{4}$$

The Eq. (4), the corresponding proton group peak positions x_k, and the normalization $\rho(x=150\text{ mm})=1$, determine the dispersion function. A plot of $[\rho(x)-1]$ is shown in Fig. 7. In addition to the statistical uncertainty in the location of each point, an error in E_1 introduces a systematic uncertainty in the slope. However, in practice, this systematic error is negligible.

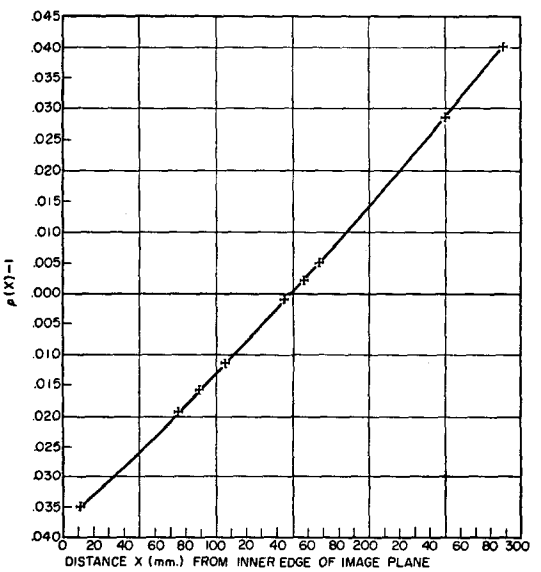

FIG. 7. The function $[\rho(x)-1]$ as a function of distance across the image plane.

[22] Enge, Buechner, and Sperduto, Phys. Rev. 88, 963 (1952).

Measurement of the Incident Beam Energy

If in Eq. (1), both Q and Q^* are known, the incident beam energy at midfoil may be determined from the expression

$$E_1=\frac{Q-r^2qQ^*-T.}{R+\Theta}. \tag{5}$$

Determined in this way E_1 will have high accuracy only when the two comparison groups have different mass, since otherwise both $[Q-r^2qQ^*-T]$ and $(R+\Theta)$ are nearly zero and have large relative errors. The special case $Q^*=0$, $M_2^*=2$, $M_2=1$ was discussed qualitatively above. Although Θ in Eq. (5) depends on E_1, it does so insensitively, so that it is sufficient to substitute in Θ the nominal beam energy.

The analysis of Eq. (5) for the effect of errors in the measured quantities is straightforward and will be omitted. One result, that an error in a deuteron Q^* is propagated with a factor $\simeq 2$ into an error in E_1, makes clear why the case $Q^*=0$ is most important. An error in the proton Q enters with a factor $\simeq 1$, and uncertainties in Q, the angles, peak separations and target thickness are in a typical case all of importance. At best the beam energy may be determined to within about ± 5 kev at 7.8 Mev.

VII. RELATIVE DIFFERENTIAL CROSS SECTIONS

While the gross features of the angular distributions in stripping and pickup reactions are understood on the basis of the Butler theory,[23] there is reason to believe that further information about nuclear interactions can be obtained by careful and systematic examination of deviations from the theory. In addition, measurements of the absolute or even relative intensity of a group, and the determination of natural widths for virtual levels, often permit important qualitative conclusions concerning the wave function of a nuclear state.

Corrections Associated with Detector Slit Width

An angular distribution for a particle group consists in the measurement, as a function of the analyzer magnet angle, of the ratio of counts in the group focused at the center of the analyzer image plane to counts in a monitor in the scattering chamber fixed with respect to the deuteron beam. When photographic plates are used as detectors, the total number of particles in the group is obtained as a matter of course. When a counter telescope is used, the number of counts obtained per unit monitor count corresponds to only a fraction of the group, the fraction depending on the ratio of the width S of the slit in front of the counter to the half-width $x_{\frac{1}{2}}$ of the lateral spread of the particle group at the image plane. Unfortunately, $x_{\frac{1}{2}}$ varies with the mean energy of the group and thus with the magnet angle. The correction which must be applied to the angular distribution data on this account can be deduced in the following way. The counting rate of the counter telescope is observed as a function of the Larmor precession frequency f of the nuclide used with the nuclear moment fluxmeter. Since the momentum P of the particles focused at the midline of the image plane is proportional to f, from Eq. (2) the observed half-width can be expressed in millimeters by the relation

$$x_{\frac{1}{2}}'(\text{mm})=(2.71\times 10^{-4})^{-1}\Delta f/f_{\max}$$

where Δf is the half-width of the line in frequency units, and $f_{\max}$ is the frequency at the peak of the group. On the assumption that the line shape is Gaussian, the true half-width $x_{\frac{1}{2}}$ may be deduced from S and $x_{\frac{1}{2}}'$ through the relation

$$\operatorname{erf}\left[\frac{(\ln 2)^{\frac{1}{2}}S}{x_{\frac{1}{2}}}\right]=\operatorname{erf}\left[\frac{(\ln 2)^{\frac{1}{2}}(x_{\frac{1}{2}}'+S)}{x_{\frac{1}{2}}}\right]-\operatorname{erf}\left[\frac{(\ln 2)^{\frac{1}{2}}(x_{\frac{1}{2}}'-S)}{x_{\frac{1}{2}}}\right].$$

The relation between the true number of counts N_t in the group to the number N_s observed with the slit S is then

$$N_s/N_t=C^{-1}=\operatorname{erf}[(\ln 2)^{\frac{1}{2}}S/x_{\frac{1}{2}}].$$

When $S\ll x_{\frac{1}{2}}$, $x_{\frac{1}{2}}'\simeq x_{\frac{1}{2}}$. When $S\gg x_{\frac{1}{2}}$, $x_{\frac{1}{2}}'\simeq S$ and the observed half-width gives little information about the true half-width. However, for this case the observed maximum counting rate N_s approaches the true number of counts N_t in the group. When there are no other groups close in energy to the group under study this limit of large slit width is normally chosen. A convenient approximate formula for the correction C which is good to $\pm 1\%$ for $(x_{\frac{1}{2}}'/S)\geq 1.3$ is

$$C=1.086\cdot\frac{(x_{\frac{1}{2}}')}{S}-0.086.$$

Owing to unsymmetrical fluctuations in the energy loss in the target,[24] and owing to a slight low-energy tail in the spectrum of the incident deuteron beam, the line shape is not a true Gaussian distribution. The error introduced on this account is small, however, particularly since it is in part compensated in the measurement of the half-width of the group.

Corrections Arising from Nonzero Angular Aperture and from Scattering in the Source

Let θ represent the deviation of an ion from the mean angle accepted by the analyzer, and let $2\theta_0$ represent the analyzer horizontal angular aperture, so that $-\theta_0\leq\theta\leq+\theta_0$. If the particles of a given reaction group are

[23] S. T. Butler, Proc. Roy. Soc. (London) **A208**, 559 (1951).

[24] For this and for other references see the review article by S. K. Allison and S. D. Warshaw, Revs. Modern Phys. **25**, 779 (1953).

produced with an angular distribution $I(\theta)=I_0 f(\theta)$, where $f(0)=1$, the number of counts N at the image plane will differ from the desired number $N_t=I_0 \cdot 2\theta_0$ for two reasons: (1) multiple scattering in the target will alter the distribution incident on the analyzer and (2) when the altered distribution is nonlinear, the parabolic term in the distribution contributes to the integral over the analyzer aperture. Both effects reduce the maxima and augment the minima in an angular distribution.

The distribution function $f(\theta)$ may be written with sufficient accuracy as $f(\theta)=1+A\theta+B\theta^2$. Except near 0° there is a negligible variation in the polar angle with vertical position at the analyzer aperture and the problem is essentially one dimensional. Scattering in the target multiplies the angular distribution $I(\theta)$ at every point across the aperture by the factor $[1+(1/2)B(\theta_d^2+\theta_p^2)]$, where θ_d and θ_p are the rms space angles of scattering resulting from traversal by incident and emergent particles respectively of the thicknesses of the target leading to and from the target midplane. Integration of the altered distribution over the aperture yields

$$N=N_t\{1+(1/3)B[\theta_0^2+(3/2)(\theta_d^2+\theta_p^2)]\}.$$

As an example, for 7.8 Mev deuterons incident on a Mylar target, $(C_{10}H_9O_4)_n$, of thickness 2.0 mg/cm², with 8.5-Mev protons emergent, $\theta_d=0.16°$ and $\theta_p=0.14°$. Since $\theta_0=1.1°$, the finite aperture effect easily dominates. This result is typical of low Z targets thin enough to give reasonable energy resolution. Even for rapidly varying stripping angular distribution with, say $B=0.05$ deg^{-2}, the correction is only 2%. That the corrections are small is verified experimentally by the fact that the measured distributions are essentially independent of target thickness.

In many distributions a near cusp occurs at 0°. The linear term in the expansion of $f(\theta)$ now yields a correction and the parabolic term may be neglected. For an analyzer aperture centered on 0°, of magnitude $\pm\theta_0$ horizontally and $\pm\phi_0$ vertically, an integral of this distribution over the aperture leads to

$$N=N_t\left\{1+(1/3)A\theta_0\left[\sec\gamma+\frac{\cot\gamma}{2}\cdot\log\tan\left(\frac{\pi}{4}+\frac{\gamma}{2}\right)-\frac{\tan^2\gamma}{2}\log\tan\frac{\gamma}{2}\right]\right\},$$

where $\gamma=\tan^{-1}(\phi_0/\theta_0)$. An exact calculation of the effect of target scattering for angles near 0° requires numerical integration. An order of magnitude estimate can be obtained by assuming an aperture of negligible vertical extent for which the aperture correction is $N=N_t[1+(A\theta_0/2)]$. The scattering correction is

$$N=N_t\{1+A\Phi(\theta_0/\Theta)+(A/2\sqrt{\pi})\Theta\exp[-(\theta_0/\Theta)^2]\}.$$

Here $\Theta=(\theta_d^2+\theta_p^2)^{\frac{1}{2}}$ and Φ is the error function.

Background

Significant background counting rate, with either photographic plates or counters, is nearly always due to entry via the analyzer ductwork of particles of the same kind as the group under study.

Ordinarily the problem is serious in only two situations: (1) in studying reaction products near 0°, when the incident deuteron beam necessarily enters the ductwork to the analyzer; and (2) in examining groups leaving the residual nucleus highly excited. In this case the background is probably an accumulation of low-energy "tails" of peaks resulting from higher energy groups. Further study of both situations is needed.

VIII. ACKNOWLEDGMENTS

The preliminary design studies for the focusing magnet were made by J. S. King, and the initial study of the performance of this magnet by L. W. Jones and K. M. Terwilliger. The field preparation for installation of the nuclear moment fluxmeter in the analyzer magnet main gap was carried out by O. M. Bilaniuk. H. M. Nye, R. H. White, and R. D. Pittman made valuable contributions to the design, fabrication, and assembly of nearly all components of the system.